

---

# Work-Function Engineering in Novel High Al Composition $\text{Al}_{0.72}\text{Ga}_{0.28}\text{N}/\text{AlN}/\text{GaN}$ HEMTs

Guowang Li, Tom Zimmermann, Yu Cao, Chuanxin Lian, Xiu Xing, Ronghua Wang,  
Patrick Fay, Huili Grace Xing, Debdeep Jena\*  
Department of Electrical Engineering, University of Notre Dame,  
Notre Dame, IN 46556, \* Email: djena@nd.edu

Enormous progress has been made in low Al composition (<40 %) AlGa<sub>N</sub>/Ga<sub>N</sub> HEMTs for high power and high frequency applications [1]. For scaling down to deep sub-micrometer dimensions, high Al composition AlGa<sub>N</sub> barrier can offer higher two-dimensional electron gas (2DEG) density and lower sheet resistance than low Al composition AlGa<sub>N</sub> [2]. Pure AlN barriers cause high contact resistance due to their wide band gap (6.2 eV) [3]. Compared to lattice-matched AlInN barriers, the higher band gap and conduction band offset of high Al composition AlGa<sub>N</sub> barrier can result in lower gate tunneling current [4]. In this work we report the device characteristics of novel high Al composition  $\text{Al}_{0.72}\text{Ga}_{0.28}\text{N}/\text{AlN}/\text{GaN}$  HEMTs. By combining ALD technology, threshold voltage control by work-function engineering is demonstrated for the first time.

The heterostructures were grown by MBE. As shown in Fig.1, as-grown 72 % AlGa<sub>N</sub>/Ga<sub>N</sub> heterostructures exhibited deep hexagonal stripes, and low mobility. By inserting an ultrathin AlN spacer, the surface morphology was dramatically improved, and the room temperature electron mobility increased by one order of magnitude. HEMTs were fabricated on these high quality heterostructures with an AlN spacer. A 4 nm ALD Al<sub>2</sub>O<sub>3</sub> gate dielectric was used in the gate stack (Fig. 2). Device isolation mesas were formed by BCl<sub>3</sub>/Cl<sub>2</sub>-based reactive ion etching. Ti/Al/Ni/Au metal stacks were deposited by electron-beam evaporation and then spike annealed to obtain ohmic contacts. Gates with various lengths were defined by electron-beam lithography. Al/Au and Ni/Au gate metals were deposited on adjacent devices on the same sample to investigate work-function engineering. A schematic of device structures and a SEM image of a 0.5 μm gate length device are shown in Fig.2. Due to unoptimized ohmic metal stacks and annealing conditions, the contact resistance (~2.4 Ω · mm) was high. Fig.3 shows the scaling trend of drain current density with decreasing Ni/Au gate lengths. All Ni/Au gate HEMTs exhibit weakly E-mode operation. For the 3-μm-long Ni/Au gate HEMTs with V<sub>GS</sub> = 0 V, I<sub>DS</sub>/I<sub>GS</sub> stays below 10/2.1 μA/mm at V<sub>DS</sub> = +100 V, indicating respectable breakdown characteristics. The transfer characteristics of 2-μm-long Ni/Au HEMTs with varying temperature (80 K ≤ T ≤ 400 K) are shown in Fig.4. While maintaining high on/off ratios, the subthreshold slope (SS) increases linearly with temperature and keeps consistently 16 mV/decade higher than the thermal limit. The corresponding extracted interface trap densities decreased with temperature (Fig. 4). The knee voltages did not change appreciably with varying temperature, indicating that device performance is currently limited by contact resistance. Room temperature transfer characteristics of gate and drain currents and DC transfer characteristics of 1-μm-long Al/Au and Ni/Au gate HEMTs are shown in Fig. 5. The ~0.8 V threshold voltage shift by different work function gate metals is clearly observed [Fig. 5(b)]. For 1-μm-long Ni/Au gate HEMTs, the drain induced barrier lowering (DIBL) factor was extracted to be ~20 mV/V with V<sub>DS</sub> ranging from 5 mV to 5 V, confirming long channel characteristic. The current gain cut-off frequency and power gain cutoff frequency  $f_{Tf_{max}}$  was measured to be 6.8/4.9 GHz and 6/12 GHz for 1-μm-long Al/Au and Ni/Au gate HEMTs, respectively. At high gate overdrives, both 0.5-μm-long Al/Au and Ni/Au gate HEMTs show ~0.5 A/mm current drive.

In conclusion, device performance of high Al composition  $\text{Al}_{0.72}\text{Ga}_{0.28}\text{N}/\text{AlN}/\text{GaN}$  HEMTs with ALD Al<sub>2</sub>O<sub>3</sub> dielectric is reported. Employing different gate metals, the threshold voltages were shifted by ~0.8 V in 0.5-μm-long HEMTs, which indicates an unpinned Fermi level at the ALD Al<sub>2</sub>O<sub>3</sub>/  $\text{Al}_{0.72}\text{Ga}_{0.28}\text{N}$  interface. With lower contact resistances, high Al AlGa<sub>N</sub> HEMTs are well suited for further lateral and vertical scaling to push towards high frequency E/D-mode performance.

[1] U. Mishra *et al*, *Proc. IEEE*, **90**, 1022, (2002).

[2] Y. Pei *et al*, *IEEE Electron Device Lett.*, **29**, 300, (2008).

[3] T. Zimmermann *et al*, *Phys. Stat. Sol. C*, **5**, 2030, (2008).

[4] R. Butté *et al*, *J. Phys. D: Appl. Phys.*, **40**, 6328 (2007).

\* This work has been supported by AFOSR (Kitt Reinhardt) and DARPA (NEXT program, John Albrecht, HR0011-10-C-0015).

\* The views, opinions, and/or findings contained in this article/presentation are those of the author/presenter and should not be interpreted as representing the official views or policies, either expressed or implied, of the Defense Advanced Research Projects Agency or the Department of Defense.

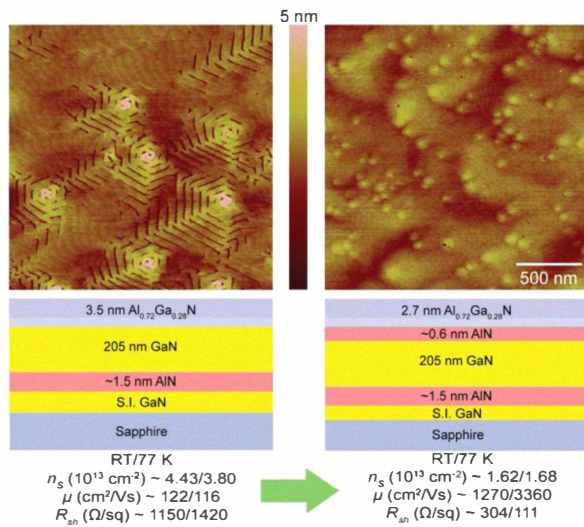


**Fig.1** Inserting AlN spacer removes hexagonal stripes shown in AFM images and improves 2DEG mobility.

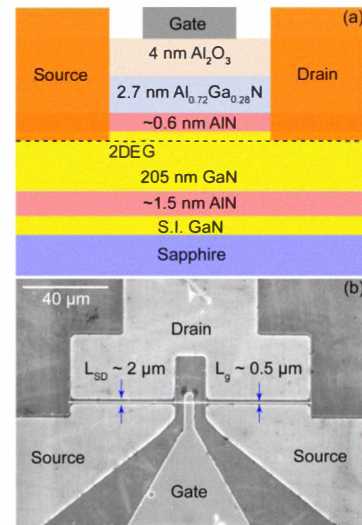


**Fig.2** (a) Schematic device structure; (b) SEM image of a 500 nm gate length HEMT.

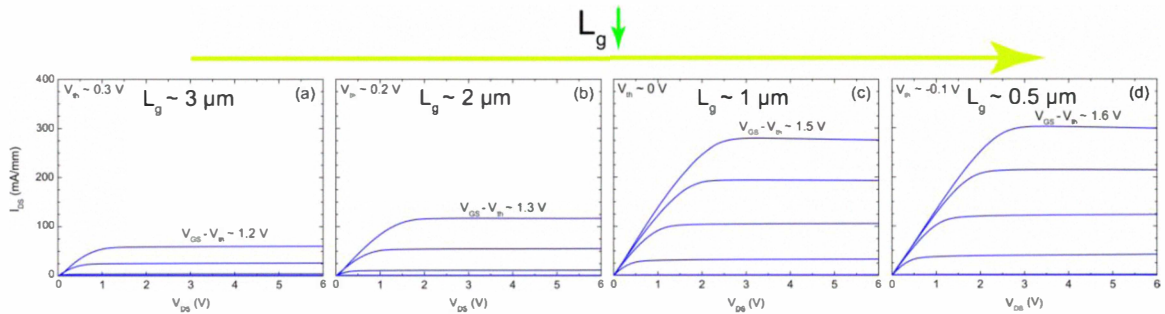


**Fig. 3** Output characteristics of Ni/Au gate HEMTs with decreasing gate length at  $T = 300 \text{ K}$ .  $V_{GS}$  is swept in 0.5 V steps and  $W_g = 50 \mu\text{m}$  for all four devices.  $L_{GS}/L_{SD} = 1 \mu\text{m}/5 \mu\text{m}$ ,  $1 \mu\text{m}/4 \mu\text{m}$ ,  $0.5 \mu\text{m}/2.1 \mu\text{m}$  and  $0.55 \mu\text{m}/2.2 \mu\text{m}$  for  $L_g = 3, 2, 1$  and  $0.5 \mu\text{m}$ , respectively.

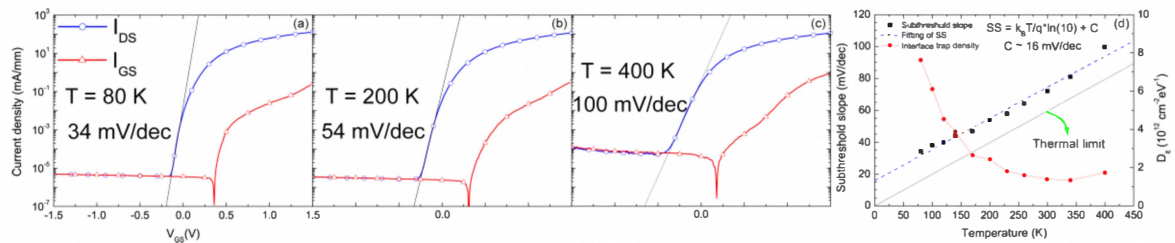


**Fig. 4** Transfer characteristics of 2- $\mu\text{m}$ -long Ni/Au HEMTs at different temperature.  $W_g = 50 \mu\text{m}$ ,  $L_{GS}/L_{SD} = 1 \mu\text{m}/4 \mu\text{m}$  and  $V_{DS} = +3 \text{ V}$ . Temperature dependence of subthreshold slopes shown and corresponding interface trap densities are shown in (d).

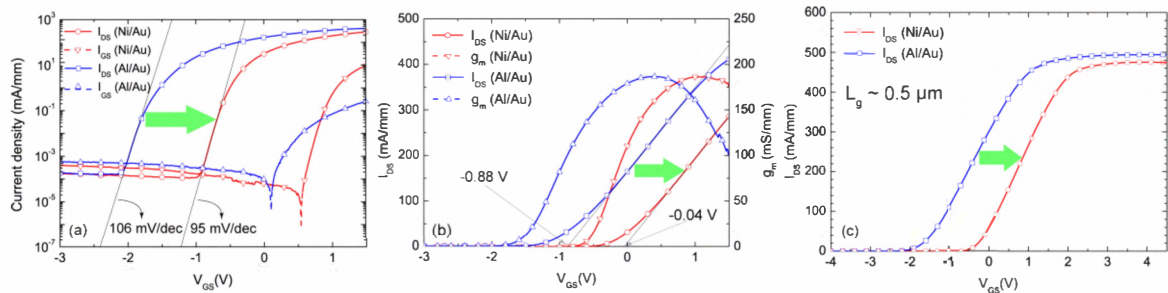


**Fig. 5** Transfer characteristics of gate and drain currents (a) and DC transfer characteristics (b) at 300 K for 1- $\mu\text{m}$ -long Al/Au and Ni/Au gate HEMTs.  $W_g = 50 \mu\text{m}$ ,  $V_{DS} = +3 \text{ V}$ ;  $L_{GS}/L_{SD} = 0.3 \mu\text{m}/2.2 \mu\text{m}$  and  $0.5 \mu\text{m}/2.1 \mu\text{m}$  for Al/Au and Ni/Au gate HEMTs, respectively.  $\sim 0.8 \text{ V}$  threshold voltage shift is shown in (b). (c) Current drive can reach  $\sim 0.5 \text{ A/mm}$  at high gate bias.  $W_g = 50 \mu\text{m}$ ,  $V_{DS} = +5 \text{ V}$ ;  $L_{GS}/L_{SD} = 0.74 \mu\text{m}/2.3 \mu\text{m}$  and  $0.55 \mu\text{m}/2.2 \mu\text{m}$  for Al/Au and Ni/Au gate HEMTs, respectively.